PCCP

Cite this: *Phys. Chem. Chem. Phys.*, 2012, **14**, 2065–2069

www.rsc.org/pccp

PAPER

Tunable ferromagnetism in assembled two dimensional triangular graphene nanoflakes

Xiaowei Li and Qian Wang*

Received 21st September 2011, Accepted 5th December 2011
DOI: 10.1039/c2cp22997h

Triangular graphene nanoflakes (TGFs), due to their novel magnetic configurations, can serve as building blocks to design new magnetic materials. Based on spin polarized density functional theory, we show that the two dimensional (2D) structures composed of zigzag-edged TGFs linked by 1,3,5-benzenetriyl units (TGF_N–C_6H_3) are ferromagnetic. Their magnetic moments can be tuned by changing the size and edge termination of TGFs, namely magnetic moments increase linearly with the size of TGFs, and double hydrogenation of the edge carbon atoms can significantly enhance stability of the ferromagnetic states. The dynamic stability of the assembled 2D structures is further confirmed by frequency calculations. The characteristic breathing mode is identified where the frequency changes with the inverse square root of the TGFs width, which can be used to identify the size of TGF_N–C_6H_3 in Raman experiments. This study provides new pathways to assemble 2D ferromagnetic carbon materials.

Since the discovery of the giant magnetoresistance effect,[1,2] extensive research has been devoted to finding new materials for spintronic devices. The hotly pursued carbon-based magnetic materials are potential candidates for such applications.[3–7] Unlike conventional spintronic materials where magnetism is due to d or f electrons, magnetism in carbon-based structures originates from p electrons, having weak spin–orbit coupling and hyperfine interactions[8] which are the main channels of relaxation and decoherence of electron spins. These properties together with the remarkable electronic and mechanical properties of carbon-based materials make them promising for transport of spin-polarized currents as well as for spin-based quantum information processing. Among the diverse carbon-based nanostructures, graphene nano ribbons (GNRs), carbon chains (CCs) and triangular graphene nanoflakes (TGFs) have recently attracted considerable attention due to their novel electronic and magnetic configurations.[9–23] It has been found that the two opposite edges of GNRs show antiferromagnetic (AFM) coupling,[9–13] and a finite CC with even (with bare ends) or odd (with hydrogenated ends) number of carbon atoms only has a total magnetic moment of 2.0 μ_B regardless of its length.[14,15] From the point of view of ferromagnetism and tunability, zigzag-edged TGF is unique. Different from GNRs, the magnetic moments at its three edges are coupled ferromagnetically.[16–22] It also differs from CCs, the total magnetic moment of TGF can be tuned by changing its size and it obeys Lieb's theorem.[24] Such novel properties promote the TGFs as promising building blocks for new magnetic carbon-based structures. However, the challenge is how to assemble the TGFs with long range ferromagnetic order for practical applications. A possible paradigm in this direction, following the strategy used in organic magnetic materials, is to use ferromagnetic coupling (FC) units to link the TGFs. In organic chemistry, 1,3,5-benzenetriyl is a well-known FC unit for versatile ferromagnetic (FM) structures.[25] Thus, a question arises: does this FC unit work for the TGFs to achieve a long range ferromagnetic order? In this paper, with the aim of designing ferromagnetic porous carbon-based materials, a first principles study of geometries, electronic structures, vibrational and magnetic properties of the 2D periodic structures composed of zigzag-edged TGFs and 1,3,5-benzenetriyls with and without hydrogen terminations has been performed. We show that the assembled structures are all FM, and their magnetic moments can be tuned by changing the size as well as the edge termination. In experiments, TGFs have been fabricated by cutting graphene sheets with electron beam irradiation and etching techniques.[26,27] The 2D TGFs based porous structures theoretically designed here could be obtained by various advanced cutting techniques.

A 2D structure unit cell has been generated using one zigzag-edged TGF_N as a spin-containing component and one 1,3,5-benzenetriyl (C_6H_3 ring) as a FC linker, having them in the same plane (defined as the x–y plane) and introducing 12 Å vacuum space along the z direction to prevent the unit cell to interact with its image. The periodic porous geometry is schematically plotted in Fig. 1(a), where the number (N) of hexagons along one edge of the TGF is used to identify the unit cell size, labeled as TGF_N–C_6H_3. To study the magnetic coupling between the unit cells, a supercell consisted of the 2×2 unit cells is used. The equilibrium structures, the total

Center for Applied Physics and Technology, College of Engineering, Peking University, Beijing 100871, China.
E-mail: qianwang2@pku.edu.cn

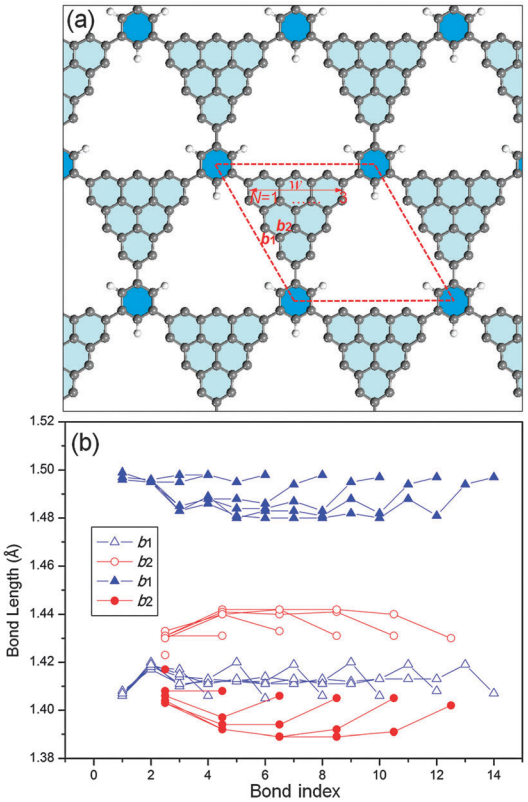

Fig. 1 (a) Geometric structure of the assembled TGF_3–C_6H_3. The rhombus consisting of dashed lines represents a unit cell. w and N are the width and number of hexagons along one edge, and b_1 and b_2 stand for the edge and inner bonds of the TGF, respectively. (b) Bond lengths of b_1 and b_2 corresponding to the C–C bond index along the width direction for the singly (hollow symbols) and doubly (solid symbols) hydrogenated TGF_N–C_6H_3 (N = 2 to 7) structures.

energies, and the electronic and magnetic properties were calculated using the spin polarized density function theory and the Vienna *ab initio* simulation package (VASP).[28] The exchange and correlation potentials were computed by using the generalized gradient approximation (GGA) with PBE form.[29] All the atoms were fully relaxed by using a conjugate-gradient algorithm. The convergence for energy and force is 0.01 meV and 0.001 eV $Å^{-1}$, respectively, and the energy cutoff was set as 400 eV. For the Brillouin zone sampling, (13 × 13 × 1) to (3 × 3 × 1) (the number is reduced gradually by integer 2) Monkhorst–Pack k-point meshes were used for the unit cells with size N from 2 to 7, respectively. For each of the supercells (N = 2 to 7), we computed the total energies corresponding to both the FM and AFM spin alignments. The energy difference ΔE between the FM and AFM states, defined as $\Delta E = E_{AFM} - E_{FM}$, was calculated to determine the preferred magnetic coupling. The phonon frequencies at the Γ point are obtained by the *ab initio* force constant method,[30] the Raman spectrum is calculated by the empirical bond polarizability model.[31,32]

In order to determine the most stable hydrogenated edge structure of a zigzag edged TGF, we calculated the C–H termination formation energy ε_H, which is defined as: $\varepsilon_H = \frac{1}{N_H}(E_{total} - E_0 - \frac{N_H}{2}E_{H_2})$, where E_{total} is the total energy of the edge hydrogenated TGF, E_0 is the energy of the bare TGF, E_{H_2} is the energy of a single H_2 molecule, and N_H is the number of H atoms in the hydrogenated TGF. We have considered several different types of edge terminations, including bare (note as z_0), single (z_1), double (z_2) hydrogenations and two more complicated edge structures, namely z_{211} (one doubly hydrogenated edge-site and two singly hydrogenated adjacent edge-sites) and z_{121} (one doubly hydrogenated edge-site and two singly hydrogenated separate edge-sites). Taking the TGF_3 as an example, we found that the z_{111} edge structure of the TGF_3 has the lowest formation energy, which is different from the situation in GNRs, where the z_{211} type hydrogenation is the most stable edge structure.[33] The formation energies of the z_{211} and z_{121} edge structures of TGFs are higher than that of the z_{111} type structure by 0.60 and 0.57 eV H^{-1}, respectively. Therefore, in this study we have used the three ideal edge terminations, namely the z_0, z_1 and z_2 edge types to study the effect of edge termination on the magnetic properties of the assembled TGFs structures. We have also changed the size N of TGF_Ns from 2 to 7 to explore the size dependence.

We began with the analysis of geometrical structures of the assembled TGF_N–C_6H_3 (N = 2 to 7). In a zigzag-edged TGF_N, the carbon atoms at the edges with dangling bonds are defined as A sites, and their neighboring sites are defined as B sites. The numbers of A and B sites in the TGF_N are given by: $N_A = (N^2 + 5N)/2$, $N_B = (N^2 + 3N + 2)/2$, respectively. There are $2N$ C–C bonds (b_1) in one zigzag edge which are connected with the inner carbon atoms by ($N - 1$) bonds (b_2), as shown in Fig. 1(a). Geometry optimization and total energy calculations were carried out for all the structures. The changes of calculated bond lengths of b_1 and b_2, labeled as d_{b_1} and d_{b_2}, respectively, with respect to the C–C bond index along the width direction for the singly and doubly hydrogenated TGF_N–C_6H_3 are plotted in Fig. 1(b). We note that both d_{b_1} and d_{b_2} are quite different in these two different hydrogenated systems due to having different sp^2 and sp^3 hybridized edges, respectively. For the singly hydrogenated systems, the two end bond lengths of d_{b_1} and d_{b_2} are smaller than those in the middle bonds excepting the smaller structures with N = 2 and 3, where d_{b_1} is smaller than d_{b_2}. While the inside C–C bond length is not sensitive to edge hydrogenation and is close to that of 1.42 Å in graphene sheets. On the other hand, for the doubly hydrogenated frameworks, the two end bond lengths are larger than the middle bonds (not including N = 2 and 3, either), and d_{b_1} is larger than d_{b_2}. This is because that sp^3 hybridization significantly elongates the bond length of the b_1 bond (in the range of 1.48–1.50 Å) but decreases the length of the b_2 bond. For the bare-edged systems, d_{b_1} (d_{b_2}) is decreased (increased) by about 0.02 Å, as compared to those in the singly hydrogenated structures.

We then studied the magnetic properties of the 2D structures. It was found that all the systems are magnetic, and each of them carries a magnetic moment that is linearly increased

Table 1 Total magnetic moment (in μ_B/unit cell) for the 2D TGF_N–C_6H_3 (N = 2 to 7) structures with the different edge terminations

Size N	2	3	4	5	6	7
Bare	7	11	15	19	23	27
Single H	1	2	3	4	5	6
Double H	5	7	9	11	13	15

with the size N and depends on the edge terminations. The magnetic moments for the systems with different size N and different hydrogenated edges are listed in Table 1. For the bare, singly and doubly hydrogenated systems, the total moments are found to be $(4N - 1)$, $(N - 1)$ and $(2N + 1)$ μ_B per unit cell, respectively. This is because for the bare-edged structures, the $3N$ edge C atoms have sp hybridization, resulting in $3N$ dangling bonds. Each of them contributes a moment of 1 μ_B. Therefore, the total magnetic moment is $(N_A - N_B + 3N)\mu_B$, *i.e.* $(4N - 1)\mu_B$. For the singly hydrogenated systems, all the C atoms are in sp^2 bonding similar to those in graphene. The difference between the number of C atoms at A and B sites is: $(N_A - N_B) = (N - 1)$. Accordingly, the magnetic moment is $(N - 1)\mu_B$. While the double hydrogenation turns the edge states into sp^3 hybridization, which have no contribution to the magnetic moment. This leads to a total moment of $|N_A - N_B - 3N|\mu_B$, *i.e.* $(2N + 1)\mu_B$.

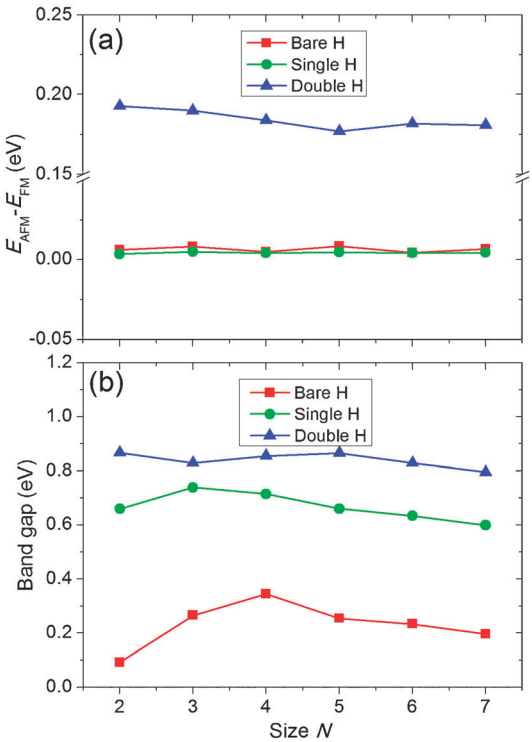

Fig. 2 Changes of energy difference ΔE (a) and band gap (b) with respect to the size N for the assembled 2D structures with different edge hydrogenations.

To further study the magnetic coupling between the unit cells, we calculated the energy difference ΔE between the FM and AFM spin alignments for all the systems studied above. The calculated results are given in Fig. 2(a). It was found that the FM state always has lower energy than the AFM one for all the configurations. ΔE shows little dependence on the size N, but it is sensitive to the edge termination. For the bare and singly hydrogenated systems, ΔE is small and is in the range of 5–10 meV per unit cell. The FM states, however, lie lower in energy by about 0.2 eV per unit cell than the AFM ones for the doubly hydrogenated structures. We see that the double hydrogenation significantly enhances the magnetic stability of the structures.

We then explored the origin of the different magnetic behaviors. To this end, we plotted the spin density iso-surfaces of the TGF_3–C_6H_3 with the different edge terminations, as shown in Fig. 3. We see, although the magnetic moment for all the structures mainly comes from the 2p orbitals of C atoms, for the structures with the bare and singly hydrogenated TGFs, the net spin density is mainly localized on the A sites of TGFs and the spins on B sites are small. Since the 1,3,5-benzenetriyl connects the TGFs through B sites, accordingly the induced spin polarization on the FC unit is weak [see Fig. 3(a) and (b)], and the energy difference ΔE is small. However, the situation is different in the doubly hydrogenated system, where the B sites carry large magnetic moments, which strongly polarize the FC units [see Fig. 3(c)]. Therefore, the FC unit becomes more effective in mediating the magnetic interaction between the TGFs, resulting in the large energy difference ΔE. We also note that the spins at B sites always polarize antiferromagnetically the C atoms at 1,3,5 sites in the 1,3,5-benzenetriyl unit, leading to the spins at 2, 4, 6 sites of the unit parallel to those at the B sites. In this way the FM coupling between the TGFs is achieved.

The band structures and density of states (DOS) of the newly designed 2D structures were also calculated, as shown in Fig. 4, to gain a deeper understanding of the magnetism. The difference between the singly and doubly hydrogenated systems can be seen clearly. Fig. 4(a) shows that in the singly

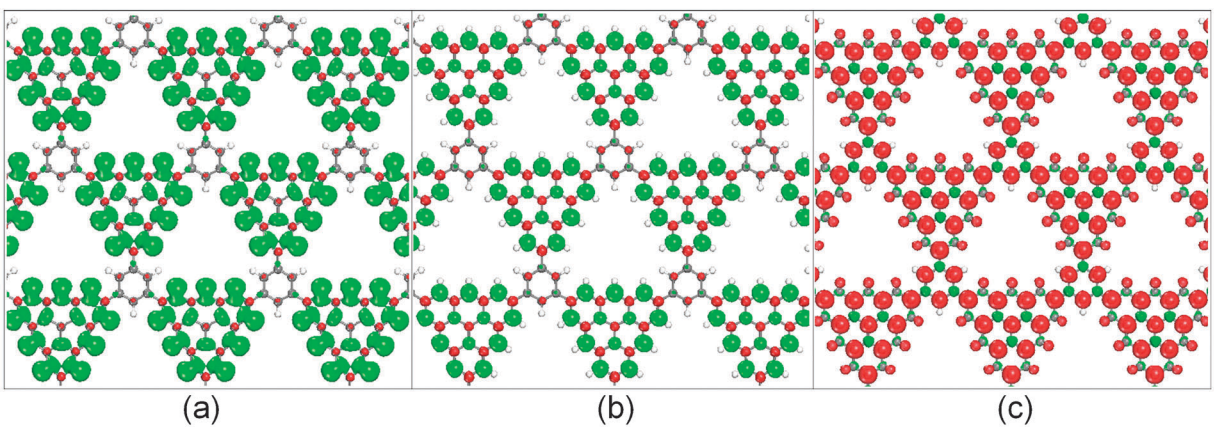

Fig. 3 Calculated spin density $(\rho_\uparrow - \rho_\downarrow)$ iso-surfaces of the 2D assembled structure with the barely (a), singly (b) and doubly hydrogenated (c) TGF_3–C_6H_3.

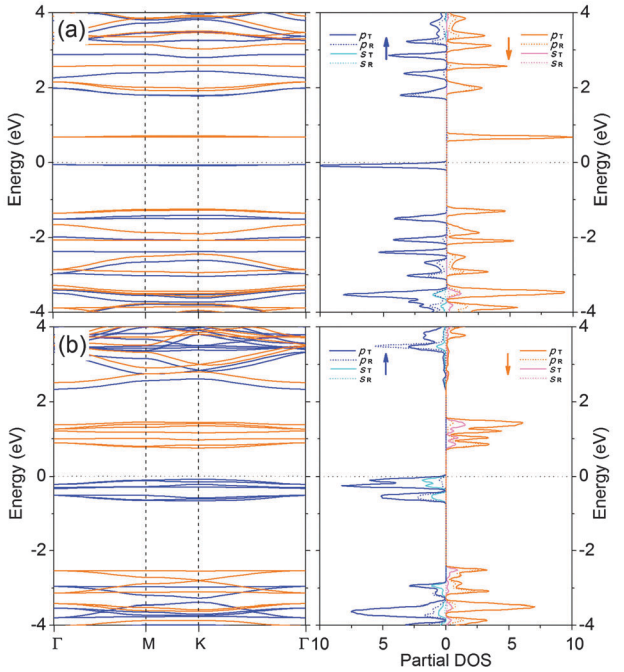

Fig. 4 Band structures and the corresponding partial DOSs of the 2D structures with the singly (a) and doubly (b) hydrogenated TGF_3–C_6H_3. Dark and light lines in band structures (left) represent spin up and spin down, respectively. The subscripts T and R in partial DOS (right) are for the contributions from the TGF and the C_6H_3 ring, respectively.

hydrogenated system, there are two-split bands near the Fermi level E_F that are dominated by the C 2p orbitals of the TGFs. The 1,3,5-benzenetriyl has minor contribution to the bands. Accordingly its ability of mediating the magnetic coupling between the TGFs is weak. While for the system with doubly hydrogenated edges [see Fig. 4(b)], there are seven spin-split bands near the E_F, which are governed by the 2p orbitals of C atoms on both the TGFs and the 1,3,5-benzenetriyl. The partial DOS shows that in addition to the 2p orbitals, the s orbitals of H atoms in the TGFs also make small contributions to the bands near E_F. Thus, the s–p and p–p orbitals hybridizations make the 1,3,5-benzenetriyl play the role of FC unit in mediating the magnetic coupling between the TGFs, leading to the strong FM coupling. Furthermore, we also found that all the calculated structures have similar split bands and they are all direct-band-gap semiconductors. The change of band gap with size N is plotted in Fig. 2(b). For a given size N, the band gap increases going from bare to single and double hydrogen terminations. It is in the range of 0.10–0.35, 0.60–0.74, and 0.79–0.87 eV for the bare, singly, and doubly hydrogenated systems, respectively.

Finally, we have calculated the frequencies of phonons at the Γ point for all the assembled 2-D structures (N = 2 to 7) to determine their stability. Not any unstable mode was found. Therefore, all the structures are dynamically stable. Based on the frequency calculations, we further studied their Raman Spectra, which is well known as an ideal technique to study the geometrical and physical properties of materials because of its nondestructive advantage. The calculated Raman spectra for the structures with their edges in doubly hydrogenated are given in Fig. 5(a). It shows clearly that there is a characteristic mode, in which the frequency decreases with increasing the size N. The corresponding atomic displacement (N = 3 as an example) and the frequency changes with respect to the inverse square root of TGFs width ($1/\sqrt{w}$, w in Å) are plotted in Fig. 5(b) and (c), respectively. We see that this peculiar mode corresponds to the unitary in-plane vibration which is similar to the radial breathing mode (RBM) of single-walled carbon nanotubes.[34] Here, we define this peculiar mode as in-plane

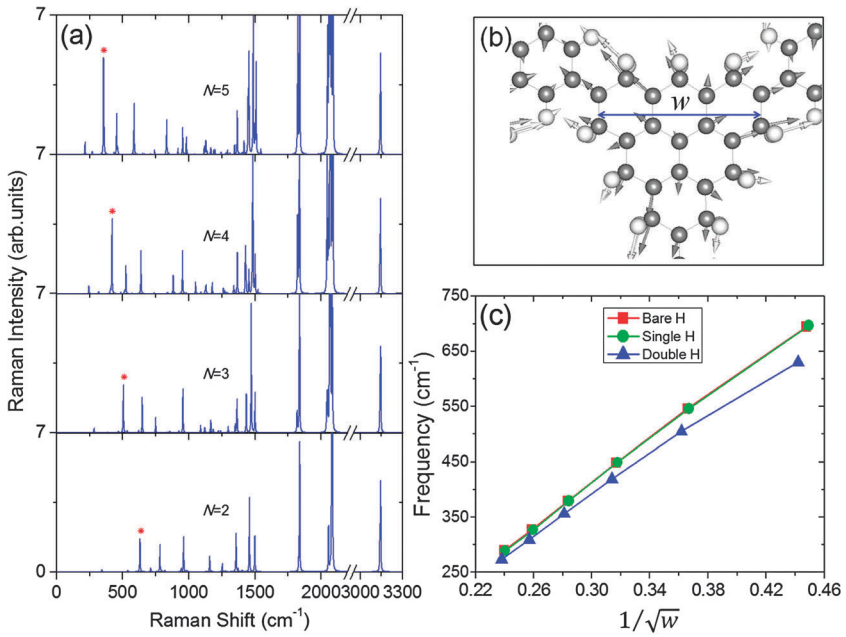

Fig. 5 (a) Non-resonant Raman spectra of the doubly hydrogenated TGF_N–C_6H_3 frameworks (N = 2 to 5). The breathing modes are labeled with red stars. (b) Atomic displacement of the breathing mode. The solid arrows represent the vibrational vectors. (c) Breathing mode frequency *vs.* the inverse square root of TGFs width w for the different edge hydrogenations.

breathing mode (BM). It was found that the changes of the BM frequencies in bare and singly hydrogenated structures are nearly in a same line, and their frequencies are larger than those of the doubly hydrogenated ones. We find that the changes of frequencies with the width w can be fitted by $\omega = a/\sqrt{w} + b$, here ω and b are in the unit of cm^{-1}, w is in Å, and a is in cm^{-1} $Å^{1/2}$, namely

$\omega = (2038.78/\sqrt{w} - 200.54)$ (for the bare/single hydrogenation)

$\omega = (1878.81/\sqrt{w} - 172.75)$ (for the double hydrogenation).

The difference between them is caused by the elongation of C–C bonds due to sp^3 hybridization in edge states of the doubly hydrogenated structures. The elongated C–C bonds decrease the force constants of the TGF_N–C_6H_3 and results in the smaller slope and frequencies. Therefore, the BM frequency is useful to determine the structure of TGF_N–C_6H_3.

In summary, we have investigated the geometries, electronic structures, magnetic properties, dynamic stability and Raman spectra of the assembled 2D porous structures using the TGFs as building blocks and the 1,3,5-benzenetriyl units as linkers. We find that the resulting systems are FM semiconductors with the band gaps changing from 0.1 to 0.9 eV. Edge termination can tune the strength of magnetic coupling between the TGFs. The 1,3,5-benzenetriyl unit becomes more effective in mediating the magnetic coupling when the edges of TGFs are doubly hydrogenated. The frequency calculations confirmed that the assembled structures are dynamically stable. In addition, the linear relationships are found for the change of magnetic moment with size N and the change of BM frequency with the inverse square root of TGFs width w. The long-range ferromagnetism together with the kinetic stability, flexible tunability, and the homogenous porosity makes the assembled structures very promising in many potential applications. The present study provides theoretical insight into the applications of the novel graphene nanoflakes in design of new magnetic materials. We hope it can stimulate further experimental studies.

Acknowledgements

This work is supported by grants from the National Natural Science Foundation of China (Grant No. NSFC-11174014) and the National Grand Fundamental Research 973 Program of China (Grant No. 2012CB921404).

Notes and references

1 M. N. Baibich, J. M. Broto, A. Fert, F. Nguyen Van Dau, F. Petroff, P. Etienne, G. Creuzet, A. Friederich and J. Chazelas, *Phys. Rev. Lett.*, 1988, **61**, 2472.
2 G. Binasch, P. Grünberg, F. Saurenbach and W. Zinn, *Phys. Rev. B: Condens. Matter*, 1989, **39**, 4828.
3 S. Krompiewski, *Cent. Eur. J. Phys.*, 2010, **9**, 369.
4 W. Y. Kim and K. S. Kim, *Acc. Chem. Res.*, 2010, **43**, 111.
5 S. Krompiewski, R. Gutiérrez and G. Cuniberti, *Phys. Rev. B: Condens. Matter*, 2004, **69**, 155423.
6 S. Athanasopoulos, S. W. Bailey, J. Ferrer, V. M. G. Suárez, C. J. Lambert, A. R. Rocha and S. Sanvito, *J. Phys.: Condens. Matter*, 2007, **19**, 042201.
7 Y.-T. Zhang, H. Jiang, Q.-F. Sun and X. C. Xie, *Phys. Rev. B: Condens. Matter*, 2010, **81**, 165404.
8 O. V. Yazyev, *Rep. Prog. Phys.*, 2010, **73**, 056501.
9 H. Lee, Y.-W. Son, N. Park, S. Han and J. Yu, *Phys. Rev. B: Condens. Matter*, 2005, **72**, 174431.
10 D. Gunlyckea, J. Li, J. W. Mintmire and C. T. White, *Appl. Phys. Lett.*, 2007, **91**, 112108.
11 H. Şahin and R. T. Senger, *Phys. Rev. B: Condens. Matter*, 2008, **78**, 205423.
12 A. R. Rocha, T. B. Martins, A. Fazzio and A. J. R. da Silva, *Nanotechnology*, 2010, **21**, 345202.
13 Y.-W. Son, M. L. Cohen and S. G. Louie, *Phys. Rev. Lett.*, 2006, **97**, 216803.
14 Z. Y. Li, W. Sheng, Z. Y. Ning, Z. H. Zhang, Z. Q. Yang and H. Guo, *Phys. Rev. B: Condens. Matter*, 2009, **80**, 115429.
15 X. F. Fan, L. Liu, J. Y. Lin, Z. X. Shen and J.-L. Kuo, *ACS Nano*, 2009, **3**, 3788.
16 W. L. Wang, S. Meng and E. Kaxiras, *Nano Lett.*, 2008, **8**, 241.
17 M. Ezawa, *Phys. Rev. B: Condens. Matter*, 2009, **79**, 241407.
18 H. Şahin, R. T. Senge and S. Ciraci, *J. Appl. Phys.*, 2010, **108**, 074301.
19 J. Akola, H. P. Heiskanen and M. Manninen, *Phys. Rev. B: Condens. Matter*, 2008, **77**, 193410.
20 M. R. Philpott, S. Vukovic, Y. Kawazoe and W. A. Lester, Jr., *J. Chem. Phys.*, 2010, **133**, 044708.
21 P. Potasz, A. D. Güçlü, O. Voznyy, J. A. Folk and P. Hawrylak, *Phys. Rev. B: Condens. Matter*, 2011, **83**, 174441.
22 J. Fernández-Rossier and J. J. Palacios, *Phys. Rev. Lett.*, 2007, **99**, 177204.
23 L. Yang, C.-H. Park, Y.-W. Son, M. L. Cohen and S. G. Louie, *Phys. Rev. Lett.*, 2007, **99**, 186801.
24 E. H. Lieb, *Phys. Rev. Lett.*, 1989, **62**, 1201.
25 M. M. Wienk and R. A. J. Janssen, *J. Am. Chem. Soc.*, 1997, **119**, 5398.
26 C. Jin, H. Lan, L. Peng, K. Suenaga and S. Iijima, *Phys. Rev. Lett.*, 2009, **102**, 205501.
27 A. Chuvilin, J. C. Meyer, G. Algara-Siller and U. Kaiser, *New J. Phys.*, 2009, **11**, 083019.
28 G. Kresse and J. Furthmuller, *Phys. Rev. B: Condens. Matter*, 1996, **54**, 11169.
29 J. P. Perdew, K. Burke and M. Ernzerhof, *Phys. Rev. Lett.*, 1996, **77**, 3865.
30 G. Kresse, J. Furthmüller and J. Hafner, *Europhys. Lett.*, 1995, **32**, 729.
31 R. Saito, T. Takeya, T. Kimura, G. Dresselhaus and M. S. Dresselhaus, *Phys. Rev. B: Condens. Matter*, 1999, **59**, 2388.
32 J. Martín and S. Montero, *J. Chem. Phys.*, 1984, **80**, 4610.
33 T. Wassmann, A. P. Seitsonen, A. M. Saitta, M. Lazzeri and F. Mauri, *Phys. Rev. Lett.*, 2008, **101**, 096402.
34 A. Jorio, R. Saito, J. H. Hafner, C. M. Lieber, M. Hunter, T. McClure, G. Dresselhaus and M. S. Dresselhaus, *Phys. Rev. Lett.*, 2001, **86**, 1118.